

Fast Track to Winning Tickets: Repowering One-Shot Pruning for Graph Neural Networks

Yanwei Yue*, Guibin Zhang*[†], Haoran Yang, Dawei Cheng[‡]

Department of Computer Science and Technology, Tongji University
{2053965, bin2003, 2010498, dcheng}@tongji.edu.cn

Abstract

Graph Neural Networks (GNNs) demonstrate superior performance in various graph learning tasks, yet their wider real-world application is hindered by the computational overhead when applied to large-scale graphs. To address the issue, the Graph Lottery Hypothesis (GLT) has been proposed, advocating the identification of subgraphs and subnetworks, *i.e.*, winning tickets, without compromising performance. The effectiveness of current GLT methods largely stems from the use of iterative magnitude pruning (IMP), which offers higher stability and better performance than one-shot pruning. However, identifying GLTs is highly computationally expensive, due to the iterative pruning and retraining required by IMP. In this paper, we reevaluate the correlation between one-shot pruning and IMP: while one-shot tickets are suboptimal compared to IMP, they offer a *fast track* to tickets with a stronger performance. We introduce a one-shot pruning and denoising framework to validate the efficacy of the *fast track*. Compared to current IMP-based GLT methods, our framework achieves a double-win situation of graph lottery tickets with **higher sparsity** and **faster speeds**. Through extensive experiments across 4 backbones and 6 datasets, our method demonstrates 1.32% – 45.62% improvement in weight sparsity and a 7.49% – 22.71% increase in graph sparsity, along with a 1.7 – 44 \times speedup over IMP-based methods and 95.3% – 98.6% MAC savings. The source code is available at <https://github.com/yanweiyue/FastGLT>.

1 Introduction

Graph Neural Networks (GNN) (Kipf and Welling 2016; Hamilton, Ying, and Leskovec 2017) have recently become the predominant approaches for various graph-related learning challenges, including node classification (Velickovic et al. 2017; Cheng et al. 2023; Wang et al. 2023a, 2024), link prediction (Zhang and Chen 2018, 2019), and graph classification (Ying et al. 2018; Zhang et al. 2018; Fang et al. 2024). Nonetheless, the significant computational challenges primarily arise from the over-parameterized GNN weights that are equipped with dense connections, as well as from the large-scale graph samples as input. These factors impede efficient feature aggregation during the training and inference

*These authors contributed equally.

[†]Project Lead, [‡]Corresponding Author

Copyright © 2025, Association for the Advancement of Artificial Intelligence (www.aaai.org). All rights reserved.

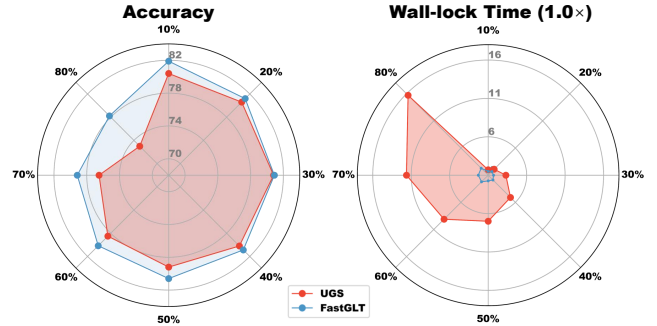


Figure 1: (**Left**) Accuracy (\uparrow) of UGS and FastGLT on Cora+GAT, with fixed weight sparsity $s_\theta = 90\%$ and graph sparsity $s_g \in \{10\%, 20\%, \dots, 80\%\}$ (**Right**) Relative wall-clock time (\downarrow) compared to a single baseline training for searching GLTs. Note that FastGLT requires far less wall-lock time to obtain subnetwork/subgraph with better performance than multiple rounds of IMP employed in UGS.

processes of GNNs (Jin et al. 2021; Zhang et al. 2024b). Worse still, these intrinsic limitations curtail the application of GNNs in large-scale scenarios, particularly under resource-restricted conditions.

Prudently reflecting on prior research, the majority of efforts to tackle this inefficiency have concentrated on either (1) *reducing the network’s parameters* or (2) *sparsifying the input graph* (Zhang et al. 2024a; Chen, Ma, and Xiao 2018; Zhang et al. 2024c,b). The first class typically employs methods like quantization (Tailor, Fernandez-Marques, and Lane 2020), pruning (Zhou et al. 2021), and distillation (Chen et al. 2020) to streamline GNN parameters. The second category involves leveraging graph sampling or sparsification techniques to reduce the computational demands caused by dense graphs (Chen, Ma, and Xiao 2018; Eden et al. 2018; Li et al. 2020b). Recently, the Graph Lottery Ticket hypothesis (GLT) (Chen et al. 2021b) takes the first step to unify the above two research lines. Briefly put, GLT aims to identify a *graph lottery ticket*, *i.e.*, a combination of a *core subgraph* and a *sparse subnetwork* with admirable performance for accelerating GNN training and inference process. Such a hypothesis is inspired by the Lottery Ticket Hypothesis (LTH) (Frankle and Carbin 2018),

which posits that sparse but performant subnetworks exist in a dense network with random initialization, like *winning tickets* in a lottery pool. Considering its exceptional potential, subsequent research has developed GLT from both theoretical (Bai et al. 2022; Wang et al. 2023b) and algorithmic perspective (Zhang et al. 2024b; Wang et al. 2023d, 2022; You et al. 2022).

As one of the most well-established graph and weight pruning approaches, the success of GLT is attributed to the application of IMP, whose fundamental concept is to involve iteratively pruning and retraining the model, methodically eliminating a small percentage of the remaining weights in each cycle, and persisting until the target pruning ratio is achieved. Unfortunately, **the computational cost of IMP becomes excessively high as the targeted pruning ratio rises and pruned graph volume grows** (You et al. 2022; Zhang et al. 2021), as shown in Fig. 1 (*Right*). To decrease computational expenses, several efficient one-shot magnitude pruning (OMP) methods have been introduced (Lee, Ajanthan, and Torr 2018; Wang, Zhang, and Grosse 2020; Ma et al. 2021), which directly prune the model to the desired sparsity level. However, they (1) typically exhibit a notable performance degradation compared to IMP (Ma et al. 2021; Frankle et al. 2020) and (2) mainly focus on weight pruning, and their performance in the context of joint pruning (graph/GNN) within the GLT context remains unexplored and unknown.

In this work, we take the first step to explore the feasibility of utilizing one-shot pruning in place of IMP within the GLT context, aiming to break the persistent challenge that the performance of one-shot pruning has been inferior to IMP. Towards this end, we introduce a One-shot Pruning and Denoising Framework toward Fast Track Graph Lottery Tickets (termed **FastGLT**). Technically, **FastGLT** initially obtains tickets at a sparsity level close to the target through one-shot pruning, followed by denoising these tickets based on gradient and degree metrics to achieve performance comparable to traditional GLT derived from IMP. Our rationale for this approach stems from a straightforward motivation: Although subnetworks/subgraphs revealed by one-shot pruning are less optimal than those from IMP, the gap between these suboptimal tickets and IMP’s winning tickets is minimal and exhibits consistent patterns. Therefore, these one-shot tickets represent a *fast track* to winning tickets. By denoising them, we can swiftly locate GLTs with significantly lower computational costs than those with IMP (shown in Fig. 1). Our contributions can be summarized as follows:

- We re-evaluate one-shot pruning within the context of graph lottery tickets, hypothesizing and empirically validating a *fast track* whereby one-shot tickets directly lead to high-performing winning tickets.
- We introduce a one-shot pruning and denoising framework (**FastGLT**) for efficiently identifying GLTs. **FastGLT** forgoes the expensive IMP steps in traditional ones, leveraging one-shot tickets as a fast track toward winning tickets accompanied by performance that is in no way inferior to that of IMP.
- Extensive experiments on 6 datasets and 4 GNN architec-

tures show that (i) **FastGLT** achieves significant improvements in both weight sparsity (5.82% – 25.48% ↑) and graph sparsity (3.65% – 17.48% ↑) compared to current state-of-the-art GLT methods (Chen et al. 2021b; Wang et al. 2023d), and (ii) **FastGLT** demonstrates substantial efficiency, achieving a 1.7-44× speedup over IMP-based GLTs and 95.3% – 98.6% MAC savings.

2 Preliminary & Motivation

2.1 Notations

We consider an undirected graph $\mathcal{G} = \{\mathcal{V}, \mathcal{E}\}$, with \mathcal{V} as the node set and \mathcal{E} the edge set of \mathcal{G} . The feature matrix of \mathcal{G} is represented as $\mathbf{X} \in \mathbb{R}^{N \times F}$, where $N = |\mathcal{V}|$ signifies the total number of nodes in the graph. The feature vector for each node $v_i \in \mathcal{V}$, with F dimensions, is denoted by $x_i = \mathbf{X}[i, \cdot]$. An adjacency matrix $\mathbf{A} \in \{0, 1\}^{N \times N}$ is utilized to depict the inter-node connectivity, where $\mathbf{A}[i, j] = 1$ indicates an edge $e_{ij} \in \mathcal{E}$, and 0 otherwise. Let $f(\cdot; \Theta)$ represent a GNN model with Θ as its parameters. For instance, a two-layer GCN is formulated as:

$$\mathbf{Z} = f(\{\mathbf{A}, \mathbf{X}\}; \Theta) = \text{Softmax}(\hat{\mathbf{A}}\sigma(\hat{\mathbf{A}}\mathbf{X}\Theta^{(0)})\Theta^{(1)}), \quad (1)$$

where \mathbf{Z} denotes the output, $\hat{\mathbf{A}} = \hat{\mathbf{D}}^{-\frac{1}{2}}(\mathbf{A} + \mathbf{I}_n)\hat{\mathbf{D}}^{-\frac{1}{2}}$ is the normalized adjacency matrix, $\tilde{\mathbf{A}} = \mathbf{A} + \mathbf{I}_n$, $\hat{\mathbf{D}}$ is the degree matrix of $\hat{\mathbf{A}}$, $\sigma(\cdot)$ is an activation function, and $\Theta^{(k)}$ is the weight matrix at the k -th layer.

2.2 Graph Lottery Ticket

Given an input graph \mathcal{G} and a GNN model $f(\cdot; \Theta)$, let $\mathcal{G}_{\text{sub}} = \{\mathbf{A} \odot \mathbf{M}_g, \mathbf{X}\}$ be a subgraph of \mathcal{G} and $f_{\text{sub}}(\cdot; \Theta \odot \mathbf{M}_\theta)$ be a subnetwork of $f(\cdot; \Theta)$. Here, \mathbf{M}_g and \mathbf{M}_θ are binary mask matrices for the adjacency matrix and model weights, respectively. Additionally, we can define the graph sparsity (GS) s_g and weight sparsity (WS) s_θ as follows:

$$s_g = 1 - \frac{\|\mathbf{M}_g\|_0}{\|\mathbf{A}\|_0}, \quad s_\theta = 1 - \frac{\|\mathbf{M}_\theta\|_0}{\|\Theta\|_0}, \quad (2)$$

where the $\|\cdot\|_0$ denotes the ℓ_0 norm that counts the number of non-zero elements. The graph lottery ticket (GLT) is defined with \mathcal{G}_{sub} and f_{sub} as follows:

Definition 1 (Graph Lottery Ticket). *Let \mathcal{G} represent an input graph, and let $f(\cdot; \Theta)$ denote a GNN with model parameters initialized at Θ_0 . We define a graph lottery ticket as the pair $(\mathcal{G}_{\text{sub}}, f_{\text{sub}})$, where \mathcal{G}_{sub} is a sparsified version of \mathcal{G} and f_{sub} corresponds to a sparsified model. This ticket satisfies the condition that, when trained in isolation, the performance metric $\varphi(f_{\text{sub}}(\mathcal{G}_{\text{sub}}; \Theta_0))$ is at least $\varphi(f(\mathcal{G}; \Theta_0))$, where φ denotes the test accuracy.*

We define the *extreme graph/weight sparsity* of a GLT method as the maximum graph/weight sparsity where it successfully identifies GLTs.

2.3 Motivation

Comparison & Visualization. We define the graph mask \mathbf{M}_g produced by UGS (Chen et al. 2021b) through iterative magnitude pruning as *IMP-based masks*, those pruned by

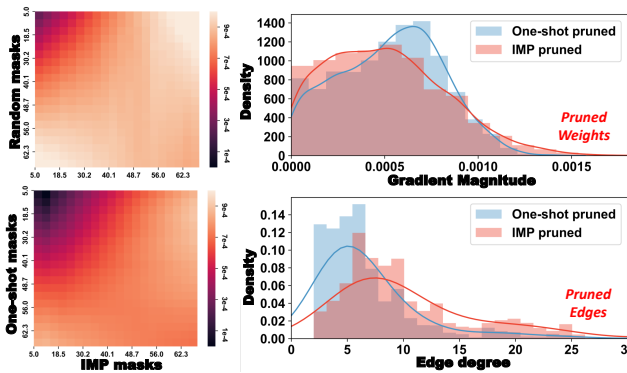


Figure 2: *(Left)* Hamming distance between masks generated by IMP, one-shot, and random sparsification methods on Cora with various graph sparsity levels $s_g \in \{5.0\%, 9.8\%, \dots, 64.2\%\}$. Notably, as sparsity increases, the distance between random and IMP masks rapidly grows, whereas one-shot masks retain greater similarity to IMP masks. *(Right)* Comparison of gradient magnitude/edge degree for weights/edges pruned by IMP or one-shot pruning.

UGS directly to the target sparsity as *one-shot masks*, and masks from random pruning as *random masks*. Fig. 2 (Left) illustrates the Hamming distance (You et al. 2022) between these masks at different sparsity levels, which can effectively reflect their differences. It is noticeable that the disparity between random and IMP masks (termed structural noise) snowballs with increasing sparsity. In contrast, the noise between one-shot and IMP masks consistently remains minimal. This prompts us to consider: *What characteristics define these structural noises?*

Empirical Validation. Further, we employed gradients (Evcı et al. 2020; Lee, Ajanthan, and Torr 2018) and edge degrees¹ (Wang et al. 2022) to visualize differences in \mathbf{M}_θ and \mathbf{M}_g between one-shot and IMP tickets, as shown in Fig. 2 (Right). Observations reveal that (1) weights pruned by IMP exhibit generally smaller gradients than those pruned one-shot, (2) degrees of edges pruned by IMP are significantly lower than those pruned one-shot. We draw an intuitive conclusion that, compared to IMP tickets, one-shot pruning’s suboptimal performance stems from mistakenly pruning a minority of weights with higher gradients and edges with lower edge degrees. A natural question arises: *can we enhance one-shot tickets’ performance by denoising structural noise using gradient- and degree-based metrics?* This will be empirically validated in the following sections.

3 Methodology

Fig. 3 illustrates the comparison between our FastGLT and IMP-based GLT methods like UGS and WD-GLT (Hui et al. 2023). Fig. 3 (Up) depicts how traditional methods iteratively prune and retrain through k iterations (each taking E epochs) to achieve a GLT at target sparsity $S\%$. Conversely, Fig. 3 (Down) shows that FastGLT employs a one-shot pruning fast track to closely approach the target sparsity, followed by a gradual denoising process to fine-tune one-shot

¹For e_{ij} , we define its edge degree as $(|\mathcal{N}(v_i)| + |\mathcal{N}(v_j)|)/2$.

tickets towards better performance. This approach requires a total computational budget of $E + D$ epochs, significantly less than IMP’s $k \times E$. In subsequent subsections, we outline in Sec. 3.1 how FastGLT acquires one-shot tickets, and then elaborate on how the gradual denoising mechanism refines these tickets in Sec. 3.2.

3.1 One-shot Pruning Tickets

As depicted above, we assign two trainable masks \mathbf{m}_g and \mathbf{m}_θ on input graph \mathcal{G} and GNN model $f(\cdot; \Theta)$ (initialized with Θ_0). Firstly, we co-optimize \mathbf{A} , Θ , \mathbf{m}_g , and \mathbf{m}_θ in an end-to-end manner using the following objective function:

$$\mathcal{L}_{os} = \mathcal{L}(f_{sub}(\{\mathbf{m}_g \odot \mathbf{A}, \mathbf{X}\}, \mathbf{m}_\theta \odot \Theta); y), \quad (3)$$

where \mathcal{L} denotes the task-irrelevant loss function (i.e., cross-entropy loss), \odot denotes element-wise multiplication and y denotes the node labels. Different from UGS (Chen et al. 2021b), we do not impose ℓ_1 regularization on \mathbf{m}_g and \mathbf{m}_θ to reduce the usage of hyperparameters. Upon completing the training, we select the optimal masks, i.e., \mathbf{m}_g and \mathbf{m}_θ from the epoch with the highest validation score, denoted as \mathbf{m}_g^* and \mathbf{m}_θ^* , for pruning.

Given the target graph sparsity s_g^{tgt} and weight sparsity s_θ^{tgt} , we avoid pruning directly to these target sparsities. This is due to the potential performance collapse (Hui et al. 2023) when targeting extremely high sparsity (e.g., 99% weight sparsity or 80% graph sparsity), which can render the model untrainable. Instead, we utilize an exponential decay function $\Psi(s) = s - \alpha s^\beta$ to pre-calculate an intermediate sparsity s_g^{inm} and s_θ^{inm} based on the target sparsities, and α and β are coefficients to adjust the output. We then zero the lowest-magnitude elements in \mathbf{m}_g^* and \mathbf{m}_θ^* w.r.t. s_g^{inm} and s_θ^{inm} in a unified manner, as outlined below:

$$\mathbf{M}^\odot = \mathbb{1}[\mathbf{m}^*] \odot \mathbb{1}[|\mathbf{m}^*| > \text{Thresholding}(\mathbf{m}^*, \Psi(s^{tgt}))], \quad (4)$$

where $\mathbf{M}^\odot \in \{0, 1\}^{|\mathbf{m}^*|}$ is either the one-shot graph mask \mathbf{M}_g^\odot or weight mask \mathbf{M}_θ^\odot , $\mathbb{1}[\cdot]$ is a binary indicator, and $\text{Thresholding}(m, s)$ denotes calculating the global threshold value at top s by sorting m in descending order.

3.2 Gradual Denoising Mechanism

As stated in (Wang et al. 2023d), traditional GLT methods irreversibly exclude elements pruned in a given iteration from subsequent considerations, leading to information loss in the pruned subgraph/subnetwork. This aligns with our assertion: one-shot masks may contain noisy and ineffective elements, while pruned parts could hold valuable structures. Towards this end, we proposed a gradual denoising mechanism, which repeatedly identifies the noisy elements in the current subgraph/subnetwork and replaces them with potential ones in the pruned components within D epochs.

Noisy Component Identification. Given the one-shot masks \mathbf{M}_g^\odot and \mathbf{M}_θ^\odot , we train the model with fixed sparse masks and a trainable graph mask \mathbf{m}_g , denoted as $f(\{\mathbf{m}_g \odot \mathbf{M}_g^\odot \odot \mathbf{A}, \mathbf{X}\}, \mathbf{M}_\theta^\odot \odot \Theta)$ with the objective function similar to Eq. 3. We execute progressive denoising over intervals spanning ΔT epochs, and the d -th epoch

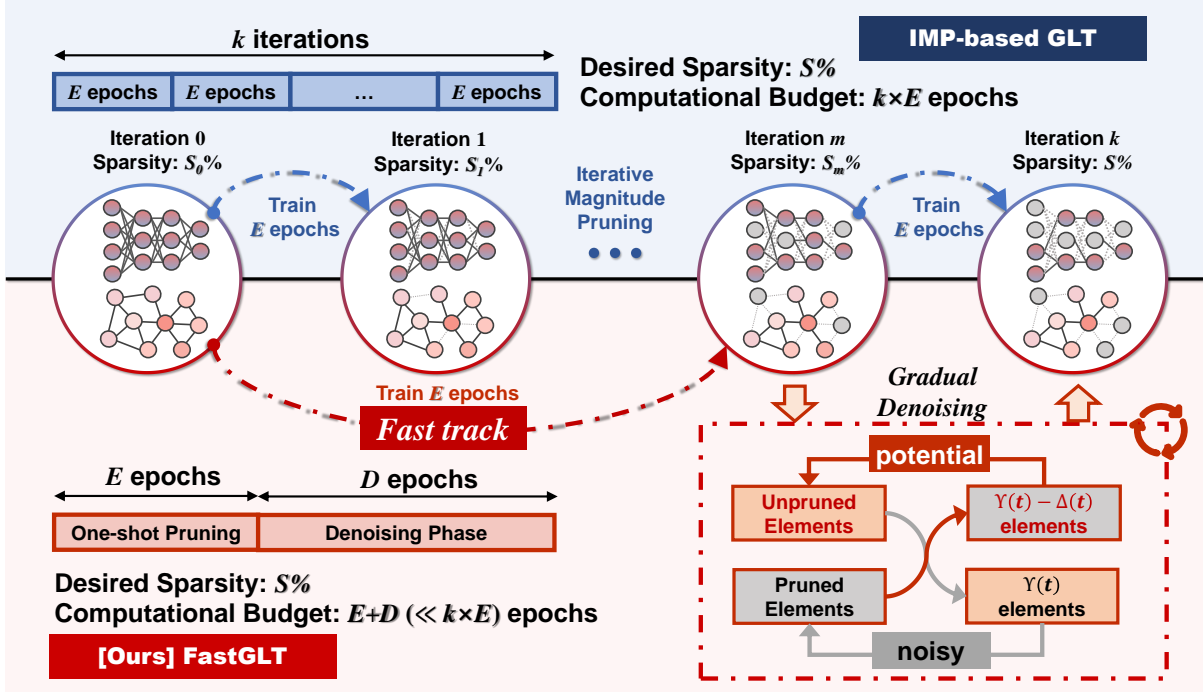


Figure 3: The detailed illustration of **FastGLT** compared to conventional IMP-based GLT. **FastGLT** replaces most of the time-consuming iterative stages with one-shot pruning as a *fast track*, and leverages a gradual denoising module to fine-tune the one-shot tickets to the target sparsity with performance in no way inferior to that of IMP.

is therefore assigned to the $[d/\Delta T]^{th}$ interval. At the end of interval μ ($1 \leq \mu \leq \lceil D/\Delta T \rceil = \mu^{end}$), analogous to traditional magnitude pruning, elements with the smallest magnitudes after ΔT training epochs with the smallest components, as defined as follows:

$$\begin{cases} \mathbf{M}_\theta^{(ns)} = \mathcal{F} \left(-|\mathbf{M}_\theta^{(\mu)} \odot \Theta_{\Delta T}|, \mathbf{N}_\theta^{(ns)} \right) \\ \mathbf{M}_g^{(ns)} = \mathcal{F} \left(-|\mathbf{M}_g^{(\mu)} \odot \mathbf{m}_g|, \mathbf{N}_g^{(ns)} \right) \end{cases} \quad (5)$$

where $\mathbf{M}_\theta^{(ns)}$ and $\mathbf{M}_g^{(ns)}$ are identified noisy weight/edges, $\mathbf{N}_\theta^{(ns)} = \#\mathbf{M}_\theta^{(\mu)} \times \Upsilon(\mu)$ and $\mathbf{N}_g^{(ns)} = \#\mathbf{M}_g^{(\mu)} \times \Upsilon(\mu)$ are the number of identified noisy weight/edges, $\mathcal{F}(m, k)$ returns the indices of top- k elements of matrix m , and $\#$ counts the number of elements in a matrix. $\Upsilon(\cdot)$ is a denoising scheduler that outputs the ratio of weights/edges to be identified between each interval. Here, we adopt the Inverse Power (Zhu and Gupta 2017; Evci et al. 2020), $\Upsilon(\mu) = \tau(1 - \mu/\mu^{end})^\kappa$, where τ denotes the initial ratio and κ is the decay factor controlling how fast the ratio decreases with intervals.

Potential Component Discovery. Slightly differently, in unearthing potentially important weights/edges, we adopt new metrics based on our observations in Sec. 2.3. Technically, for pruned weights $-\mathbf{M}_\theta^{(\mu)} \odot \Theta$, we identify those with the highest accumulated gradients as potential ones. For pruned edges $-\mathbf{M}_g^{(\mu)} \odot \mathbf{A}$, we regard those with the smallest edge degrees as potential. Notably, to gradually increase the graph/weight sparsity from the initial s_g^{inm} and s_θ^{inm} to the target s_g^{tgt} and s_θ^{tgt} , we ensure that the identified impor-

tant elements are fewer than the noisy ones by a factor of $\omega_g = \frac{\#\|\mathbf{A}\|_0 \times (s_g^{tgt} - s_g^{inm})}{\mu^{end}} \%$ or $\omega_\theta = \frac{\#\Theta \times (s_\theta^{tgt} - s_\theta^{inm})}{\mu^{end}} \%$ between each interval. The process is defined as follows:

$$\begin{cases} \mathbf{M}_\theta^{(pt)} = \mathcal{F} \left(\sum_{i=1}^{\Delta T} |\nabla_{-\mathbf{M}_\theta^{(\mu)} \odot \Theta} \mathcal{L}|, \mathbf{N}_\theta^{(pt)} \right) \\ \mathbf{M}_g^{(pt)} = \mathcal{F} \left(-(-\mathbf{M}_g^{(\mu)} \odot \mathbf{A} \odot \mathbf{S}^{(\mu)}), \mathbf{N}_g^{(pt)} \right), \end{cases} \quad (6)$$

where $\mathbf{M}_\theta^{(pt)}$ and $\mathbf{M}_g^{(pt)}$ are potentially important weight/edges discovered from pruned elements, $\mathbf{N}_\theta^{(pt)} = \#\mathbf{M}_\theta^{(\mu)} \times \Upsilon(t) - \omega_\theta$ and $\mathbf{N}_g^{(pt)} = \#\mathbf{M}_g^{(\mu)} \times \Upsilon(t) - \omega_g$ are the number of potentially important weight/edges, $\sum_{i=1}^{\Delta T} |\nabla_{-\mathbf{M}_\theta^{(\mu)} \odot \Theta} \mathcal{L}|$ calculates the accumulated gradients of pruned weights in interval μ , and \mathbf{S} is the edge degree matrix, calculated as follows:

$$\mathbf{S} = (\mathbf{D}^{-1} \mathbf{M}_g^{(\mu)} \mathbf{d}(\mathbf{D})^{-\frac{1}{2}}) (\mathbf{D}^{-1} \mathbf{M}_g^{(\mu)} \mathbf{d}(\mathbf{D})^{-\frac{1}{2}})^T, \quad (7)$$

where \mathbf{D} denotes the degree matrix of the sparsed graph $\mathbf{M}_g^{(\mu)}$ and $\mathbf{d}(\mathbf{D})$ returns the node degree vector of \mathcal{V} .

Mask Update. Now that we have identified both noisy and potential edges/weights, we proceed to update the graph/weight masks. Specifically, we remove the noisy components from the current mask and incorporate the potential ones, as detailed in the following process:

$$\mathbf{M}^{(\mu+1)} = \left(\mathbf{M}^{(\mu)} \setminus \mathbf{M}^{(ns)} \right) \cup \mathbf{M}^{(pt)}, \quad (8)$$

where $\mathbf{M}^{(\mu+1)}$ is either the updated graph mask $\mathbf{M}_g^{(\mu+1)}$ or weight mask $\mathbf{M}_\theta^{(\mu+1)}$. Note that between each interval, the

sparsity of $\mathbf{M}^{(\mu+1)}$ increases by $\left(\frac{s^{\text{tgt}} - s^{\text{inm}}}{\mu_{\text{end}}}\right)\%$ compared to $\mathbf{M}^{(\mu)}$, ensuring that the graph or network precisely reaches the target sparsity at the end of the denoising process.

During the continuous identifying and swapping process, both the network and the graph are denoised to the desired sparsity with satisfactory performance. The overall algorithm framework is showcased in Algo. 1.

4 Experiments

In this section, we conduct extensive experiments to answer the following three research questions: **(RQ1)** Can **FastGLT** effectively find graph lottery tickets? **(RQ2)** Can **FastGLT** scale up to larger-scale graphs? **(RQ3)** Does **FastGLT** genuinely accelerate the acquisition of winning tickets and inference speed compared to traditional IMP-based GLT?

4.1 Experiment Setup

Datasets. We select Cora, Citeseer, and PubMed (Kipf and Welling 2016) for node classification. For larger-scale graphs, we opt Ogbn-Arxiv/Proteins/Collab (Hu et al. 2020). For a fair comparison, we follow the datasets splitting criterion used by UGS (Chen et al. 2021b). On small-scale datasets, we use 140 (Cora), 120 (Citeseer), and 60 (PubMed) labeled nodes for training, 500 nodes for validation and 1000 nodes for testing. For OGB datasets, we follow the official splits given in (Hu et al. 2020).

Backbones & Baselines. To assess **FastGLT**’s adaptability across various GNN backbones, we employ three network structures for small-scale datasets: GCN (Kipf and Welling 2017), GIN (Xu et al. 2018) and GAT (Veličković et al. 2017). For larger-scale datasets, we utilize a 28-layer ResGCN (Li et al. 2020a). To comprehensively validate the efficiency of **FastGLT**, we select two state-of-the-art GLT methods, UGS (Chen et al. 2021b) and WD-GLT (Hui et al. 2023), alongside random pruning (RP), for comparison.

Parameter Settings. For small-scale datasets, the hidden dimension is uniformly set to 512. On OGB graphs, we adopt parameter settings similar to UGS (Chen et al. 2021b). Adam is used as the optimizer throughout. To compute intermediate sparsity, we employ $\Psi(s) = s - 0.01s^{1.2}$. The decay factor κ is set as 1 in all experiments. Detailed hyperparameter settings are provided in the Appendix.

4.2 Results on Small Graphs ($\mathcal{RQ1}$)

To answer $\mathcal{RQ1}$, we compare our **FastGLT** with UGS, WD-GLT and random pruning on three small-scale datasets for node classification tasks. Following (Wang et al. 2023c,d), toward a clearer illustration, we fix the weight sparsity to zero when investigating how accuracy evolves with the increase of graph sparsity, and vice versa. Fig. 4 illustrates the results on Cora, Citeseer, and PubMed, and we can draw the following observations (**Obs**):

Obs.1. FastGLT can find GLTs with sparser subgraph/subnetwork. It is observable that **FastGLT** consistently outperforms other GLT methods across all backbones and benchmarks, attaining improvements in weight sparsity from 1.32% to 45.62% and in graph sparsity from 7.49%

to 22.71%. Specifically, on Cora+GIN, the GLT identified by **FastGLT** achieves 28.66% graph sparsity and 89.16% weight sparsity, surpassing WD-GLT by 22.71% and 45.62% respectively.

Obs.2. FastGLT demonstrates greater robustness in graph sparsification. **FastGLT** uniquely sustains performance with rising graph sparsity, in contrast to typical GLT methods. On Citeseer+GAT, for instance, while UGS and WD-GLT sharply decline in performance beyond 70% graph sparsity, **FastGLT** remains close to baseline at nearly 90%.

4.3 Results on Large Graphs ($\mathcal{RQ2}$)

To answer $\mathcal{RQ2}$, we conduct comparative experiments on Ogbn-Arxiv, Ogbn-Proteins and Ogbn-Collab with 28-layer ResGCN (Li et al. 2020a). As showcased in Tab. 2 and Tab. 4, we can list the following observations:

Obs. 3. FastGLT can scale up to large graphs. **FastGLT** consistently identifies GLTs with weight sparsity over 70% and graph sparsity over 30% across three datasets, surpassing other methods which generally fall below 60% and 30%, respectively. Specifically, **FastGLT** can find GLT with 70.25% weight sparsity or 48.01% graph sparsity on Ogbn-Arxiv, exceeding UGS by 30.18% and 36.82%.

4.4 Efficiency Validation ($\mathcal{RQ3}$)

In this section, we compare the efficiency of **FastGLT** with previous GLT methods from two perspectives: (1) wall-clock time expended in the search for winning tickets, and (2) inference speed of the most sparse tickets discovered. From Tab. 1 and Fig. 5, we draw a conclusion that **FastGLT** achieves a dual win in GLT search time and computational savings from the following observations:

Obs.4. FastGLT can identify GLTs way faster. Specifically, UGS requires $4.0 - 28.6\times$ the duration of the original dense training to find the sparsest GLT. On GIN, WD-GLT’s average time is as high as $105.6\times$. Conversely, **FastGLT** takes only $1.63 - 4\times$ the original dense training time to find the sparsest GLT. Notably, when it comes to finding a ticket with $s_\theta = 49.7\%$, $s_g = 36.9\%$ on Ogbn-Arxiv (Fig. 5), **FastGLT** achieves 12.0x and 19.6x acceleration compared to UGS and WD-GLT, respectively.

Obs.5. FastGLT excels in obtaining more computationally efficient tickets. Besides faster speed, **FastGLT** also reduces computational load significantly. Across all GCN/GIN/GAT backbones, we achieve over 95% MAC savings, surpassing UGS and WD-GLT by 5.4% to 31.0%.

4.5 Ablation Study & Sensitivity Analysis

Validation of fast track. In this part, we validate the premise that *one-shot tickets offer a fast track to winning tickets* from two aspects: convergence speed and optimal performance. Fig. 6 (Right) demonstrates that denoising from one-shot tickets not only successfully finds winning tickets, but also offers faster convergence. Tab. 5 compares the maximum s_θ and s_g when starting from randomly initialized tickets versus one-shot tickets. Notably, denoising from random tickets results in up to a 28.94% drop in weight sparsity and a 24.17% drop in graph sparsity, highlighting the necessity of using one-shot tickets as a fast track.

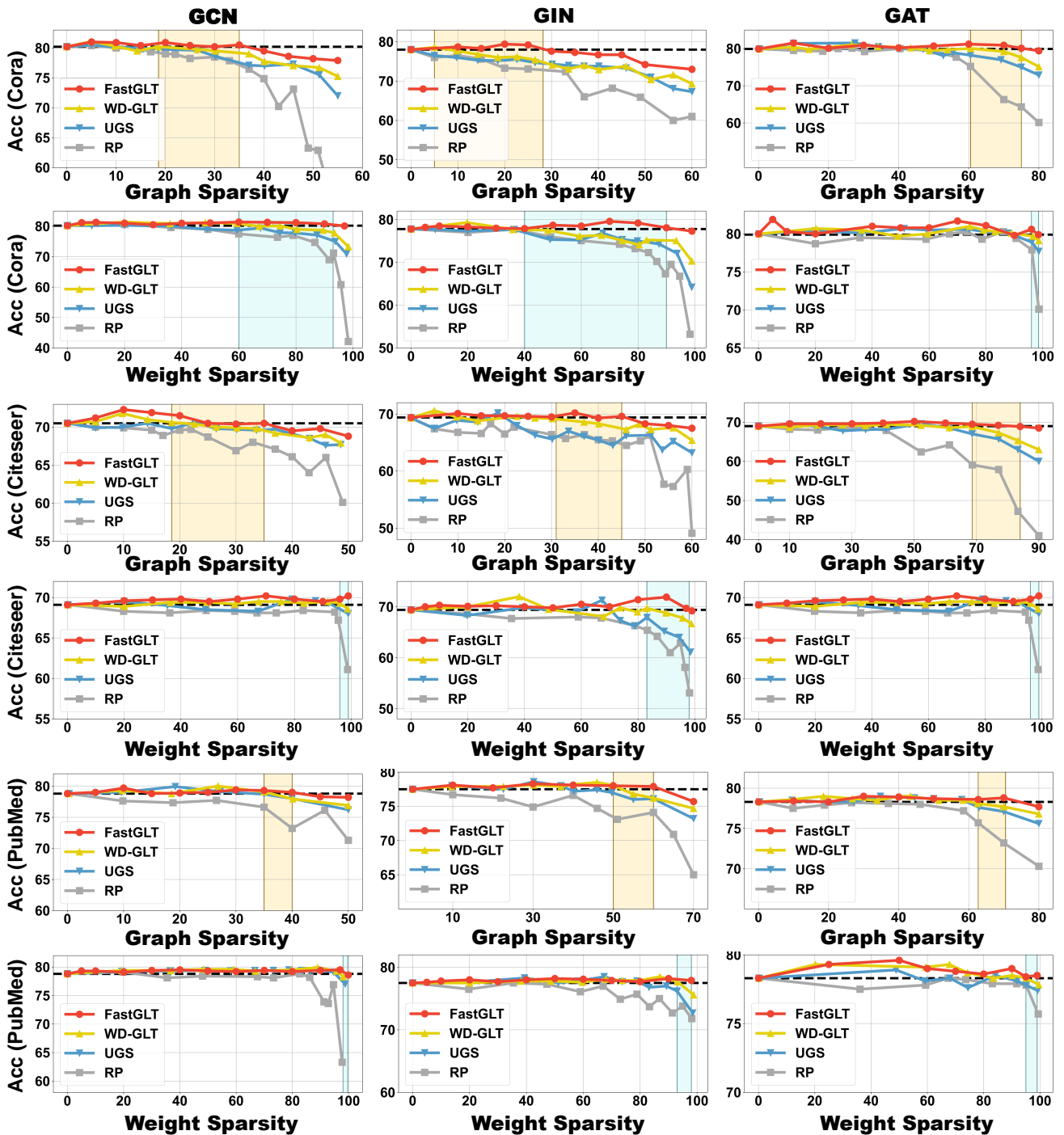


Figure 4: Results of node classification over Cora/Citeseer/PubMed with GCN/GIN/GAT backbones. Black dash lines represent the baseline performance.

Effects of denoising interval ΔT . We set graph/weight sparsity at 40%/80%, and explore FastGLT’s performances with ΔT values $\{3, 5, 10, 20, 30, 50\}$ on Ogbn-Arxiv+ResGCN and Citeseer+GAT. From Fig. 6 (Left), we observe that FastGLT’s sensitivity to ΔT is minimal, with a maximum accuracy variance of only 1.35% on Citeseer and 1.74% on Ogbn-Arxiv. The remaining parameter sensitivity

analysis is provided in the Appendix.

5 Related Work

Lottery Ticket Hypothesis Current LTH methods are categorized into *dense-to-sparse* and *sparse-to-sparse* methods, based on the initial network’s over-parameterization. The former starts with a dense network, progressively pruned

Table 1: Efficiency comparison among UGS, WD-GLT and **FastGLT**. “Acc. (%)” indicates the accuracy of the sparsest winning tickets obtained; “Obt. Time (s)” represents the wall-clock time consumed to obtain the sparsest winning ticket (for baseline, it refers to the full training time with dense network/graph); “Inference MACs (M)” refers to the inference MACs ($= \frac{1}{2}$ FLOPs) required by the identified tickets; “Relative Time (s)” refers to the time relative to the original dense training duration.

| Model | Methods | Cora | | | Citeseer | | | PubMed | | | Avg. | |
|-------|----------------|--------------|-----------|-----------|--------------|-----------|-----------|--------------|-----------|-----------|---------------|-------------|
| | | Acc. (%) | Obt. Time | Inf. MACs | Acc. (%) | Obt. Time | Inf. MACs | Acc. (%) | Obt. Time | Inf. MACs | Relative Time | MAC Savings |
| GCN | Baseline | 80.25 ± 0.18 | 21.4 | 1996M | 70.51 ± 0.06 | 41.4 | 6317M | 78.80 ± 0.14 | 1217.3 | 5077M | 1.0× | 0.0% |
| | UGS | 80.19 ± 0.06 | 76.3 | 817M | 70.66 ± 0.08 | 233.8 | 1665M | 79.01 ± 0.23 | 3500.9 | 233M | 4.0× | 75.6% |
| | WD-GLT | 80.27 ± 0.45 | 604.3 | 806M | 70.74 ± 0.51 | 801.7 | 1541M | 78.82 ± 0.33 | 5634.1 | 107M | 17.4× | 80.3% |
| | FastGLT | 80.33 ± 0.17 | 34.9 | 139M | 70.59 ± 0.12 | 89.7 | 315M | 79.11 ± 0.29 | 1366.2 | 50M | 1.63× | 95.6% |
| GIN | Baseline | 78.06 ± 0.09 | 7.3 | 2006M | 68.47 ± 0.11 | 8.6 | 6328M | 77.50 ± 0.17 | 8.8 | 5108M | 1.0× | 0.0% |
| | UGS | 78.17 ± 0.13 | 39.8 | 1284M | 68.70 ± 0.20 | 61.0 | 2073M | 77.66 ± 0.30 | 141.7 | 438M | 28.6× | 64.3% |
| | WD-GLT | 78.26 ± 0.44 | 305.4 | 1275M | 68.50 ± 0.38 | 891.4 | 1018M | 77.80 ± 0.35 | 1509.3 | 331M | 105.6× | 70.6% |
| | FastGLT | 78.32 ± 0.17 | 20.4 | 200M | 68.54 ± 0.25 | 21.3 | 126M | 77.59 ± 0.37 | 17.8 | 102M | 2.4× | 95.3% |
| GAT | Baseline | 79.95 ± 0.03 | 333.1 | 16059M | 69.12 ± 0.18 | 284.1 | 50619M | 78.35 ± 0.20 | 920.7 | 41349M | 1.0× | 0.0% |
| | UGS | 79.99 ± 0.45 | 3143.8 | 1672M | 69.23 ± 0.11 | 3434.1 | 839M | 78.39 ± 0.34 | 2960.5 | 3565M | 8.2× | 93.2% |
| | WD-GLT | 80.11 ± 0.61 | 5700.7 | 525M | 69.38 ± 1.23 | 5003.6 | 568M | 78.52 ± 0.20 | 4533.2 | 2283M | 13.2× | 96.4% |
| | FastGLT | 80.07 ± 0.37 | 525.9 | 204M | 69.30 ± 0.21 | 528.7 | 414M | 78.56 ± 0.68 | 1270.3 | 414M | 4.8× | 98.6% |

Table 2: Results on 3 large-scale OGB graphs. Each entry denotes the extreme sparsity that a certain method is capable of achieving. *Please note that extreme sparsity refers to the highest sparsity level at which GNN can achieve performance equal to the vanilla GNN.* ± corresponds to the standard deviation over 5 trials. “N/A” means GLT cannot be found.

| Dataset | Ogbn-Arxiv | Ogbn-Proteins | Ogbl-Collab |
|-------------------------|--------------|---------------|--------------|
| Graph Sparsity | | | |
| Random Pruning | N/A | 5.74 ± 2.05 | N/A |
| UGS(Chen et al. 2021b) | 11.19 ± 0.42 | 16.94 ± 0.33 | 8.20 ± 0.14 |
| WD-GLT(Hui et al. 2023) | 30.94 ± 0.51 | 22.48 ± 0.07 | 17.14 ± 0.95 |
| FastGLT (Ours) | 48.01 ± 0.17 | 34.49 ± 0.13 | 31.55 ± 0.35 |

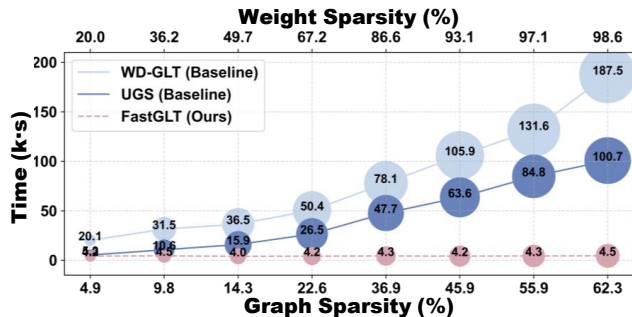


Figure 5: The wall-lock time of UGS, WD-GLT, FastGLT to locate GLTs on Ogbn-Arxiv with different s_g and s_θ .

ing to the target sparsity (Chen et al. 2021c,a; Ding, Chen, and Wang 2021), while the latter starts with a randomly initialized sparse neural network and dynamically modifies its topology during a single training run through methods like pruning-and-growing (Mocanu et al. 2018; Wang, Zhang,

and Grosse 2020; Liu et al. 2021). It’s noteworthy that our gradual denoise mechanism bears a slight resemblance to the topology-adjusting operations of sparse-to-sparse methods. However, our work differs significantly in at least two ways: (1) Current sparse-to-sparse methods focus solely on weight pruning and aren’t extendable to joint pruning. In contrast, our denoising mechanism is specifically devised based on observations of weight and graph characteristics; (2) Unlike sparse-to-sparse methods that initiate with a randomly sparse network, we start with one-shot pruning as a fast track to winning tickets, substantiated by extensive ablation studies proving its efficacy.

Graph Lottery Ticket UGS (Chen et al. 2021b) first integrated LTH’s concept into GLT research, combining *graph sparsification* with *GNN model compression*. Recent endeavors include GEBT (You et al. 2022), which revealed the existence of graph early-bird tickets. WD-GLT (Hui et al. 2023) enhanced graph pruning through an auxiliary loss function, and DGLT (Wang et al. 2023c) firstly introduced the concept of dual lottery tickets (Bai et al. 2022) to GLT paradigm. However, all these methods fall into the trap of iterative pruning, making the acquisition of GLTs resource-intensive. Conversely, leveraging the one-shot pruning as a fast track, we bypass the extensive computational demands of IMP, acquiring winning tickets much more rapidly.

6 Conclusions

In this work, we propose an effective method termed one-shot pruning and denoising framework toward fast track graph lottery tickets (**FastGLT**), which utilizes one-shot tickets as a *fast track* and denoises them to acquire sparse but performant tickets. Our work reevaluates the relationship between one-shot and IMP tickets, hypothesizing and validating that one-shot tickets can be rapidly denoised to obtain subgraphs/subnetworks that are sparser and perform compa-

rably to IMP-based tickets. This paradigm achieves a significantly faster efficiency in finding GLTs ($1.7 - 44\times$ speedup) compared to previous SOTA methods, offering new insights into how to more rapidly and effectively discover GLTs.

References

- Bai, Y.; Wang, H.; Tao, Z.; Li, K.; and Fu, Y. 2022. Dual lottery ticket hypothesis. *arXiv preprint arXiv:2203.04248*.
- Chen, J.; Ma, T.; and Xiao, C. 2018. Fastgcn: fast learning with graph convolutional networks via importance sampling. *arXiv preprint arXiv:1801.10247*.
- Chen, T.; Cheng, Y.; Gan, Z.; Liu, J.; and Wang, Z. 2021a. Data-Efficient GAN Training Beyond (Just) Augmentations: A Lottery Ticket Perspective. *Advances in Neural Information Processing Systems*, 34: 20941–20955.
- Chen, T.; Sui, Y.; Chen, X.; Zhang, A.; and Wang, Z. 2021b. A unified lottery ticket hypothesis for graph neural networks. In *International Conference on Machine Learning*, 1695–1706. PMLR.
- Chen, X.; Zhang, Z.; Sui, Y.; and Chen, T. 2021c. Gans can play lottery tickets too. *arXiv preprint arXiv:2106.00134*.
- Chen, Y.; Bian, Y.; Xiao, X.; Rong, Y.; Xu, T.; and Huang, J. 2020. On self-distilling graph neural network. *arXiv preprint arXiv:2011.02255*.
- Cheng, D.; Ye, Y.; Xiang, S.; Ma, Z.; Zhang, Y.; and Jiang, C. 2023. Anti-money laundering by group-aware deep graph learning. *IEEE Transactions on Knowledge and Data Engineering*, 35(12): 12444–12457.
- Ding, S.; Chen, T.; and Wang, Z. 2021. Audio lottery: Speech recognition made ultra-lightweight, noise-robust, and transferable. In *International Conference on Learning Representations*.
- Eden, T.; Jain, S.; Pinar, A.; Ron, D.; and Seshadhri, C. 2018. Provable and practical approximations for the degree distribution using sublinear graph samples. In *Proceedings of the 2018 World Wide Web Conference*, 449–458.
- Evcı, U.; Gale, T.; Menick, J.; Castro, P. S.; and Elsen, E. 2020. Rigging the lottery: Making all tickets winners. In *International Conference on Machine Learning*, 2943–2952. PMLR.
- Fang, J.; Zhang, G.; Wang, K.; Du, W.; Duan, Y.; Wu, Y.; Zimmermann, R.; Chu, X.; and Liang, Y. 2024. On regularization for explaining graph neural networks: An information theory perspective. *IEEE Transactions on Knowledge and Data Engineering*.
- Frankle, J.; and Carbin, M. 2018. The lottery ticket hypothesis: Finding sparse, trainable neural networks. *arXiv preprint arXiv:1803.03635*.
- Frankle, J.; Dziugaite, G. K.; Roy, D. M.; and Carbin, M. 2020. Pruning neural networks at initialization: Why are we missing the mark? *arXiv preprint arXiv:2009.08576*.
- Hamilton, W.; Ying, Z.; and Leskovec, J. 2017. Inductive representation learning on large graphs. In *Proceedings of NIPS*.
- Hu, W.; Fey, M.; Zitnik, M.; Dong, Y.; Ren, H.; Liu, B.; Catasta, M.; and Leskovec, J. 2020. Open graph benchmark: Datasets for machine learning on graphs. *arXiv preprint arXiv:2005.00687*.
- Hui, B.; Yan, D.; Ma, X.; and Ku, W.-S. 2023. Rethinking Graph Lottery Tickets: Graph Sparsity Matters. In *The Eleventh International Conference on Learning Representations*.
- Jin, W.; Zhao, L.; Zhang, S.; Liu, Y.; Tang, J.; and Shah, N. 2021. Graph condensation for graph neural networks. *arXiv preprint arXiv:2110.07580*.
- Kipf, T. N.; and Welling, M. 2016. Semi-supervised classification with graph convolutional networks. *arXiv preprint arXiv:1609.02907*.
- Kipf, T. N.; and Welling, M. 2017. Semi-supervised classification with graph convolutional networks. In *Proceedings of ICLR*.
- Lee, N.; Ajanthan, T.; and Torr, P. H. 2018. Snip: Single-shot network pruning based on connection sensitivity. *arXiv preprint arXiv:1810.02340*.
- Li, G.; Xiong, C.; Thabet, A.; and Ghanem, B. 2020a. Deepergcn: All you need to train deeper gcns. *arXiv preprint arXiv:2006.07739*.
- Li, J.; Zhang, T.; Tian, H.; Jin, S.; Fardad, M.; and Zafarani, R. 2020b. Sgcn: A graph sparsifier based on graph convolutional networks. In *Pacific-Asia Conference on Knowledge Discovery and Data Mining*, 275–287. Springer.
- Liu, S.; Yin, L.; Mocanu, D. C.; and Pechenizkiy, M. 2021. Do we actually need dense over-parameterization? in-time over-parameterization in sparse training. In *International Conference on Machine Learning*, 6989–7000. PMLR.
- Ma, X.; Yuan, G.; Shen, X.; Chen, T.; Chen, X.; Chen, X.; Liu, N.; Qin, M.; Liu, S.; Wang, Z.; et al. 2021. Sanity checks for lottery tickets: Does your winning ticket really win the jackpot? *Advances in Neural Information Processing Systems*, 34: 12749–12760.
- Mocanu, D. C.; Mocanu, E.; Stone, P.; Nguyen, P. H.; Gibescu, M.; and Liotta, A. 2018. Scalable training of artificial neural networks with adaptive sparse connectivity inspired by network science. *Nature communications*, 9(1): 2383.
- Taylor, S. A.; Fernandez-Marques, J.; and Lane, N. D. 2020. Degree-quant: Quantization-aware training for graph neural networks. *arXiv preprint arXiv:2008.05000*.
- Velickovic, P.; Cucurull, G.; Casanova, A.; Romero, A.; Lio, P.; and Bengio, Y. 2017. Graph attention networks. *stat*, 1050: 20.
- Veličković, P.; Cucurull, G.; Casanova, A.; Romero, A.; Lio, P.; and Bengio, Y. 2017. Graph attention networks. *arXiv preprint arXiv:1710.10903*.
- Wang, C.; Zhang, G.; and Grosse, R. 2020. Picking winning tickets before training by preserving gradient flow. *arXiv preprint arXiv:2002.07376*.
- Wang, K.; Li, G.; Wang, S.; Zhang, G.; Wang, K.; You, Y.; Peng, X.; Liang, Y.; and Wang, Y. 2023a. The Snowflake

Hypothesis: Training Deep GNN with One Node One Receptive field. *arXiv:2308.10051*.

Wang, K.; Liang, Y.; Li, X.; Li, G.; Ghanem, B.; Zimmermann, R.; Yi, H.; Zhang, Y.; Wang, Y.; et al. 2023b. Brave the Wind and the Waves: Discovering Robust and Generalizable Graph Lottery Tickets. *IEEE Transactions on Pattern Analysis and Machine Intelligence*.

Wang, K.; Liang, Y.; Wang, P.; Wang, X.; Gu, P.; Fang, J.; and Wang, Y. 2023c. Searching Lottery Tickets in Graph Neural Networks: A Dual Perspective. In *The Eleventh International Conference on Learning Representations*.

Wang, K.; Zhang, G.; Zhang, X.; Fang, J.; Wu, X.; Li, G.; Pan, S.; Huang, W.; and Liang, Y. 2024. The heterophilic snowflake hypothesis: Training and empowering gnn for heterophilic graphs. In *Proceedings of the 30th ACM SIGKDD Conference on Knowledge Discovery and Data Mining*, 3164–3175.

Wang, L.; Huang, W.; Zhang, M.; Pan, S.; Chang, X.; and Su, S. W. 2022. Pruning graph neural networks by evaluating edge properties. *Knowledge-Based Systems*, 256: 109847.

Wang, Y.; Liu, S.; Chen, K.; Zhu, T.; Qiao, J.; Shi, M.; Wan, Y.; and Song, M. 2023d. Adversarial Erasing with Pruned Elements: Towards Better Graph Lottery Ticket. *arXiv preprint arXiv:2308.02916*.

Xie, B.; Chang, H.; Zhang, Z.; Zhang, Z.; Wu, S.; Wang, X.; Meng, Y.; and Zhu, W. 2024. Towards Lightweight Graph Neural Network Search with Curriculum Graph Sparsification. In *Proceedings of the 30th ACM SIGKDD Conference on Knowledge Discovery and Data Mining*, KDD '24, 3563–3573. ACM.

Xu, K.; Hu, W.; Leskovec, J.; and Jegelka, S. 2018. How powerful are graph neural networks? *arXiv preprint arXiv:1810.00826*.

Ying, Z.; You, J.; Morris, C.; Ren, X.; Hamilton, W.; and Leskovec, J. 2018. Hierarchical graph representation learning with differentiable pooling. *Advances in neural information processing systems*, 31.

You, H.; Lu, Z.; Zhou, Z.; Fu, Y.; and Lin, Y. 2022. Early-bird gcn: Graph-network co-optimization towards more efficient gcn training and inference via drawing early-bird lottery tickets. In *Proceedings of the AAAI Conference on Artificial Intelligence*, volume 36, 8910–8918.

Zhang, G.; Sun, X.; Yue, Y.; Jiang, C.; Wang, K.; Chen, T.; and Pan, S. 2024a. Graph Sparsification via Mixture of Graphs. *arXiv preprint arXiv:2405.14260*.

Zhang, G.; Wang, K.; Huang, W.; Yue, Y.; Wang, Y.; Zimmermann, R.; Zhou, A.; Cheng, D.; Zeng, J.; and Liang, Y. 2024b. Graph lottery ticket automated. In *The Twelfth International Conference on Learning Representations*.

Zhang, G.; Yue, Y.; Wang, K.; Fang, J.; Sui, Y.; Wang, K.; Liang, Y.; Cheng, D.; Pan, S.; and Chen, T. 2024c. Two heads are better than one: Boosting graph sparse training via semantic and topological awareness. *arXiv preprint arXiv:2402.01242*.

Zhang, M.; and Chen, Y. 2018. Link prediction based on graph neural networks. *Advances in neural information processing systems*, 31.

Zhang, M.; and Chen, Y. 2019. Inductive matrix completion based on graph neural networks. *arXiv preprint arXiv:1904.12058*.

Zhang, M.; Cui, Z.; Neumann, M.; and Chen, Y. 2018. An end-to-end deep learning architecture for graph classification. In *Proceedings of the AAAI conference on artificial intelligence*, volume 32.

Zhang, Z.; Chen, X.; Chen, T.; and Wang, Z. 2021. Efficient lottery ticket finding: Less data is more. In *International Conference on Machine Learning*, 12380–12390. PMLR.

Zhou, H.; Srivastava, A.; Zeng, H.; Kannan, R.; and Prasanna, V. 2021. Accelerating large scale real-time GNN inference using channel pruning. *arXiv preprint arXiv:2105.04528*.

Zhu, M.; and Gupta, S. 2017. To prune, or not to prune: exploring the efficacy of pruning for model compression. *arXiv preprint arXiv:1710.01878*.

Reproducibility Checklist

Unless specified otherwise, please answer “yes” to each question if the relevant information is described either in the paper itself or in a technical appendix with an explicit reference from the main paper. If you wish to explain an answer further, please do so in a section titled “Reproducibility Checklist” at the end of the technical appendix.

This paper:

1. Includes a conceptual outline and/or pseudocode description of AI methods introduced (yes)
2. Clearly delineates statements that are opinions, hypothesis, and speculation from objective facts and results (yes)
3. Provides well marked pedagogical references for less-familiar readers to gain background necessary to replicate the paper (yes)

Does this paper make theoretical contributions? (no)

If yes, please complete the list below.

1. All assumptions and restrictions are stated clearly and formally. (yes/partial/no)
2. All novel claims are stated formally (e.g., in theorem statements). (yes/partial/no)
3. Proofs of all novel claims are included. (yes/partial/no)
4. Proof sketches or intuitions are given for complex and/or novel results. (yes/partial/no)
5. Appropriate citations to theoretical tools used are given. (yes/partial/no)
6. All theoretical claims are demonstrated empirically to hold. (yes/partial/no/NA)
7. All experimental code used to eliminate or disprove claims is included. (yes/no/NA)

Does this paper rely on one or more datasets? (yes)

If yes, please complete the list below.

1. A motivation is given for why the experiments are conducted on the selected datasets (yes/)
2. All novel datasets introduced in this paper are included in a data appendix. (NA)
3. All novel datasets introduced in this paper will be made publicly available upon publication of the paper with a license that allows free usage for research purposes. (NA)
4. All datasets drawn from the existing literature (potentially including authors' own previously published work) are accompanied by appropriate citations. (yes)
5. All datasets drawn from the existing literature (potentially including authors' own previously published work) are publicly available. (yes)
6. All datasets that are not publicly available are described in detail, with explanation why publicly available alternatives are not scientifically satisfying. (NA)

Does this paper include computational experiments? (yes)

If yes, please complete the list below.

1. Any code required for pre-processing data is included in the appendix. (yes)
2. All source code required for conducting and analyzing the experiments is included in a code appendix. (yes)
3. All source code required for conducting and analyzing the experiments will be made publicly available upon publication of the paper with a license that allows free usage for research purposes. (yes)
4. All source code implementing new methods have comments detailing the implementation, with references to the paper where each step comes from (yes)
5. If an algorithm depends on randomness, then the method used for setting seeds is described in a way sufficient to allow replication of results. (NA)
6. This paper specifies the computing infrastructure used for running experiments (hardware and software), including GPU/CPU models; amount of memory; operating system; names and versions of relevant software libraries and frameworks. (yes)
7. This paper formally describes evaluation metrics used and explains the motivation for choosing these metrics. (yes)
8. This paper states the number of algorithm runs used to compute each reported result. (yes)
9. Analysis of experiments goes beyond single-dimensional summaries of performance (e.g., average; median) to include measures of variation, confidence, or other distributional information. (yes)
10. The significance of any improvement or decrease in performance is judged using appropriate statistical tests (e.g., Wilcoxon signed-rank). (partial)
11. This paper lists all final (hyper-)parameters used for each model/algorithm in the paper's experiments. (yes)

12. This paper states the number and range of values tried per (hyper-)parameter during development of the paper, along with the criterion used for selecting the final parameter setting. (yes)

A Algorithm Workflow

We conclude the overall workflow of our **FastGLT** in Algo. 1.

Algorithm 1: Algorithm workflow of **FastGLT**

Input: $\mathcal{G} = (\mathbf{A}, \mathbf{X})$, GNN model $f(\mathcal{G}, \Theta_0)$, GNN’s initialization Θ_0 , target sparsity s_g^{tgt} for graphs and s_θ^{tgt} for weights, denoising interval ΔT , learning rate η .
Output: GLT $f(\{\mathbf{M}_g \odot \mathbf{A}, \mathbf{X}\}, \mathbf{M}_\theta \odot \Theta)$

- 1: **for** iteration $i = 1$ **to** E **do**
- 2: Forward $f_{\text{sub}}(\{\mathbf{m}_g \odot \mathbf{A}, \mathbf{X}\}, \mathbf{m}_\theta \odot \Theta)$ to compute the loss in Eq. 3.
- 3: Backpropagate to update $\Theta_{i+1} \leftarrow \Theta_i - \eta \nabla_{\Theta} \mathcal{L}_{\text{os}}$.
- 4: Update $\mathbf{m}_g^{i+1}, \mathbf{m}_\theta^{i+1} \leftarrow \mathbf{m}_g^i - \eta \nabla_{\mathbf{m}_g^i} \mathcal{L}_{\text{os}}, \mathbf{m}_\theta^i - \eta \nabla_{\mathbf{m}_\theta^i} \mathcal{L}_{\text{os}}$.
- 5: **end for**
- 6: Compute intermediate sparsity $s_g^{\text{inm}} \leftarrow \Upsilon(s_g^{\text{tgt}}), s_\theta^{\text{inm}} \leftarrow \Upsilon(s_\theta^{\text{tgt}})$.
- 7: **// One-shot Tickets.**
- 8: Set $s_g^{\text{inm}}\%$ of the lowest magnitude values in \mathbf{m}_g^E to 0 and others to 1, then obtain one-shot mask \mathbf{M}_g^\odot .
- 9: Set $s_\theta^{\text{inm}}\%$ of the lowest magnitude values in \mathbf{m}_θ^E to 0 and others to 1, then obtain one-shot mask \mathbf{M}_θ^\odot .
- 10: **// Gradual Denoising Procedure.**
- 11: Set $\mathbf{M}_g^{(1)} \leftarrow \mathbf{M}_g^\odot, \mathbf{M}_\theta^{(1)} \leftarrow \mathbf{M}_\theta^\odot$.
- 12: **for** iteration $d = 1$ **to** D **do**
- 13: Compute interval index $\mu \leftarrow \lceil d/\Delta T \rceil$.
- 14: Forward $f(\{\mathbf{m}_g \odot \mathbf{M}_g^{(\mu)} \odot \mathbf{A}, \mathbf{X}\}, \mathbf{M}_\theta^{(\mu)} \odot \Theta)$ to compute the \mathcal{L}_{os} .
- 15: Update Θ and \mathbf{m}_g accordingly.
- 16: **if** $\mu = \lceil d/\Delta T \rceil$ **then**
- 17: Identify $\mathbf{M}_\theta^{(\text{noisy})}$ and $\mathbf{M}_g^{(\text{noisy})}$ according to Eq. 5.
- 18: Identify $\mathbf{M}_\theta^{(\text{potential})}$ and $\mathbf{M}_g^{(\text{potential})}$ according to Eq. 6.
- 19: Compute $\mathbf{M}_g^{(\mu+1)}$ and $\mathbf{M}_\theta^{(\mu+1)}$ according to Eq. 7.
- 20: **end if**
- 21: **end for**

B Experimental Settings

B.1 Hyperparameter Configuration

We conclude the detailed hyperparameter configuration in Tab. 3.

C Additional Experimental Results

C.1 Additional Results on OGB Graphs

As showcased in Tab. 4, **FastGLT** consistently identifies GLTs with weight sparsity over 70% across three OGBN datasets, surpassing other methods which generally fall below 60%.

Table 3: Hyper-parameter configurations.

| Computing Infrastructures: NVIDIA Tesla V100 | | | | | | |
|--|-------|----------|-------|-------|--------------|-------|
| Param | GCN | Cora GIN | GAT | GCN | Citeseer GIN | GAT |
| E | 30 | 30 | 30 | 50 | 50 | 50 |
| D | 400 | 500 | 600 | 400 | 500 | 400 |
| lr | 0.001 | 0.001 | 0.001 | 0.001 | 0.001 | 0.001 |
| ΔT | 10 | 10 | 10 | 10 | 10 | 3 |

| Param | GCN | PubMed GIN | GAT | Arxiv | Proteins ResGCN | Collab |
|------------|-------|------------|-------|-------|-----------------|--------|
| E | 50 | 50 | 30 | 30 | 20 | 50 |
| D | 400 | 500 | 400 | 400 | 200 | 400 |
| lr | 0.001 | 0.001 | 0.001 | 0.001 | 0.001 | 0.001 |
| ΔT | 20 | 10 | 10 | 3 | 3 | 3 |

Table 4: Results on 3 large-scale OGB graphs. Each entry denotes the extreme sparsity that a certain method is capable of achieving. \pm corresponds to the standard deviation over 5 trials. ‘‘N/A’’ means GLT cannot be found.

| Dataset | Ogbn-Arxiv | Ogbn-Proteins | Ogbl-Collab |
|-------------------------|------------------------------------|------------------------------------|------------------------------------|
| Weight Sparsity | | | |
| Random Pruning | 28.72 \pm 2.38 | 17.88 \pm 3.66 | 6.14 \pm 1.54 |
| UGS(Chen et al. 2021b) | 40.07 \pm 0.16 | 33.60 \pm 0.45 | 38.32 \pm 0.24 |
| WD-GLT(Hui et al. 2023) | 63.23 \pm 0.11 | 47.23 \pm 0.18 | 59.06 \pm 1.37 |
| FastGLT (Ours) | 73.25 \pm 0.18 | 73.01 \pm 0.34 | 71.66 \pm 0.45 |

C.2 Ablation Study Results

We conduct ablation studies from three distinct perspectives: one-shot pruning(Tab. 5), denoising interval ΔT (Fig. 6), and denoising scheduler Υ (Tab. 6). Specifically, we have three observations:

- As shown in Tab. 5, one-shot tickets effectively provide a *fast track* to winning tickets.
- As shown in Fig. 6, the denoising interval ΔT does not have a significant effect on the performance of **FastGLT**.
- As shown in Tab. 6, **FastGLT** is not sensitive to denoising scheduler Υ .

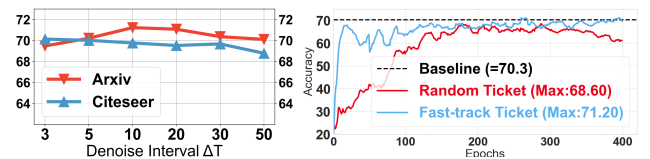


Figure 6: **(Left)** Ablation study on ΔT . We vary $\Delta T \in \{3, 5, 10, 20, 30, 50\}$ on Ogbn-Arxiv+ResGCN and Citeseer+GAT with fixed sparsity $\{s_\theta = 80\%, s_g = 40\%\}$; **(Right)** Test accuracy curves showcasing the denoising process from randomly initialized tickets and one-shot tickets on Citeseer+GCN with $\{s_g = 30\%, s_\theta = 99\%\}$.

C.3 Parameter Sensitivity Analysis

Effects of denoising interval ΔT . We set graph/weight sparsity at 40%/80%, and explore **FastGLT**’s performances with ΔT values $\{3, 5, 10, 20, 30, 50\}$ on Ogbn-Arxiv+ResGCN and Citeseer+GAT. From Fig. 6 (Left), we observe that **FastGLT**’s sensitivity to ΔT is minimal, with a

Table 5: Ablation study on denoising from randomly initialized tickets and one-shot tickets on Citeseer with GCN/GIN/GAT.

| Backbone | GCN | GIN | GAT |
|-----------------|-------|-------|-------|
| Weight Sparsity | | | |
| Random Ticket | 94.22 | 89.38 | 70.26 |
| One-shot Ticket | 99.27 | 98.33 | 99.20 |
| Graph Sparsity | | | |
| Random Ticket | 23.16 | 20.89 | 56.06 |
| One-shot Ticket | 34.17 | 45.06 | 68.97 |

Table 6: Ablation study on decay factor κ . We report performances of GCN on Cora ($s_g = 30\%$, $s_\theta = 90\%$) and Citeseer ($s_g = 40\%$, $s_\theta = 90\%$), with $\kappa \in \{1, 2, 3\}$.

| (Cora) | GCN | GIN | GAT |
|--------------|------------------|------------------|------------------|
| $\kappa = 1$ | 80.09 \pm 0.28 | 78.26 \pm 0.44 | 80.77 \pm 0.18 |
| $\kappa = 2$ | 79.84 \pm 0.23 | 78.04 \pm 0.09 | 79.80 \pm 0.11 |
| $\kappa = 3$ | 79.86 \pm 0.21 | 77.71 \pm 0.58 | 80.54 \pm 0.37 |
| (Citeseer) | GCN | GIN | GAT |
| $\kappa = 1$ | 69.26 \pm 0.04 | 70.08 \pm 0.31 | 69.88 \pm 0.12 |
| $\kappa = 2$ | 69.23 \pm 0.13 | 69.16 \pm 0.39 | 69.82 \pm 0.16 |
| $\kappa = 3$ | 69.06 \pm 0.71 | 68.14 \pm 0.15 | 68.93 \pm 0.45 |

maximum accuracy variance of only 1.35% on Citeseer and 1.74% on Ogbn-Arxiv.

Effects of denoising scheduler Υ . We evaluate the accuracy fluctuations across various GNN backbones on Cora/Citeseer when varying the decay factor κ of Inverse Power at $\{1, 2, 3\}$. The magnitude of κ is inversely related to the decay rate. Tab. 6 shows that linear decay ($\kappa = 1$) outperforms the other two decay rates, and we therefore uniformly apply $\kappa = 1$ in all experiments. Still, the maximum performance variance on Cora/Citeseer is less than 0.55%/1.94% respectively, indicating **FastGLT**'s low sensitivity to the denoising scheduler.

C.4 Comparison of One-shot Pruning and FastGLT

We have included a straightforward one-shot pruning method as an additional baseline for comparison. The experimental results, as shown in Table 7, demonstrate that FastGLT outperforms the basic one-shot approach, highlighting the benefits of our denoising framework in refining one-shot tickets to achieve higher accuracy and greater sparsity.

C.5 Extreme Sparsity of Winning Tickets

We report the extreme sparsity of Winning Tickets to enhance clarity in our results, as shown in Table 8. For One-Shot Pruning and FastGLT, we iteratively search through each sparsity level in an arithmetic sequence until a lottery ticket can no longer be found. FastGLT consistently identifies winning tickets with higher sparsity compared to the baseline, highlighting its superiority.

Table 7: Accuracy(Acc)/Extreme Sparsity(ES) Comparison of One-shot Pruning and FastGLT on Different Datasets and Backbones.

| Comparison of One-shot Pruning and FastGLT with GCN | | | | | | |
|---|--------------|--------------|--------------|--------------|--------------|--------------|
| Method | Cora | | Citeseer | | Pubmed | |
| | Acc(%) | ES(%) | Acc(%) | ES(%) | Acc(%) | ES(%) |
| Baseline | 80.25 | - | 70.51 | - | 78.80 | - |
| One-Shot | 80.09 | 15.00 | 70.65 | 25.00 | 79.06 | 25.00 |
| FastGLT | 80.33 | 35.00 | 79.11 | 35.00 | 79.11 | 40.00 |
| Comparison of One-shot Pruning and FastGLT with GAT | | | | | | |
| Method | Cora | | Citeseer | | Pubmed | |
| | Acc | ES | Acc | ES | Acc | ES |
| Baseline | 79.95 | - | 69.12 | - | 78.35 | - |
| One-Shot | 79.82 | 45.00 | 69.48 | 50.00 | 78.39 | 40.00 |
| FastGLT | 80.17 | 75.00 | 69.30 | 82.50 | 78.56 | 70.00 |

Table 8: Detailed Extreme Sparsity of Winning Tickets

| Method | GCN | | GAT | |
|----------|---------------|---------------|---------------|---------------|
| | Cora | Pubmed | Cora | Pubmed |
| One-Shot | 15.00% | 25.00% | 45.00% | 40.00% |
| WD-GLT | 18.52% | 34.65% | 60.12% | 62.45% |
| FastGLT | 35.00% | 40.00% | 75.00% | 70.00% |

D Practical Usage of GLT

Graph Lottery Ticket has been confirmed to have broad practical applications. We provide examples as follows:

- **Acceleration:** Our experiments on multiple datasets and GNNs show that FastGLT achieves an average inference speedup of 1.48x. Moreover, GLT accelerates Neural Architecture Search by applying graph sparsification combined with architecture-aware edge deletion (Xie et al. 2024).
- **Transferability:** The winning ticket can be transferred across different datasets & GNNs, eliminating the need for retraining.
- **Robustness:** GLT aids in detecting redundant and poisoned edges, enhancing input perturbation robustness.
- **Federated Learning(FL) Data Compression:** In FL, GLT obtains sparse structures from local GNNs, reducing the parameter load sent to the central server.

E Dataset and Backbone

E.1 Graph datasets statistics

We conclude the dataset statistics in Tab. 9 and Tab. 10.

Table 9: Graph datasets statistics (Part 1).

| Dataset | Nodes | Edges | Avg. Degree |
|---------------|---------|------------|-------------|
| Cora | 2,708 | 5,429 | 3.88 |
| Citeseer | 3,327 | 4,732 | 1.10 |
| PubMed | 19,717 | 44,338 | 8.00 |
| Ogbn-Arxiv | 169,343 | 1,166,243 | 13.77 |
| Ogbn-Proteins | 132,534 | 39,561,252 | 597.00 |
| Ogbl-Collab | 235,868 | 1,285,465 | 10.90 |

Table 10: Graph datasets statistics (Part 2).

| Dataset | Features | Classes | Metric |
|---------------|----------|---------|----------|
| Cora | 1,433 | 7 | Accuracy |
| Citeseer | 3,703 | 6 | Accuracy |
| PubMed | 500 | 3 | Accuracy |
| Ogbn-ArXiv | 128 | 40 | Accuracy |
| Ogbn-Proteins | 8 | 2 | ROC-AUC |
| Ogbl-Collab | 128 | 2 | Hits@50 |

E.2 Performance Metrics

Accuracy represents the ratio of correctly predicted outcomes to the total predictions made. The ROC-AUC (Receiver Operating Characteristic-Area Under the Curve) value quantifies the probability that a randomly selected positive example will have a higher rank than a randomly selected negative example. Hit@50 denotes the proportion of correctly predicted edges among the top 50 candidate edges.

E.3 Efficiency Metrics

To evaluate the efficiency of sparse graphs generated by different sparsifiers, we employ two key metrics: MACs (Multiply-Accumulate Operations) and GPU inference latency (measured in milliseconds). MACs are a theoretical indicator of the model’s inference speed, based on FLOPs (Floating Point Operations Per Second). Although `SpMM` is theoretically faster than `MatMul` according to MACs/FLOPs, this advantage is not always evident in practice due to `SpMM`’s irregular memory access pattern. To better understand the practical performance of our approach, we also measure the GPU latency in milliseconds.

E.4 Train-val-test Splitting of Datasets.

To rigorously verify the effectiveness of `FastGLT`, we unify the dataset-splitting strategy across all GNN backbones and baselines. As for node classification tasks of small- and medium-size datasets, we utilize 140(Cora), 120 (Citeseer) and 60 (PubMed) labeled data for training, 500 nodes for validation and 1000 nodes for testing. The data splits for Ogbn-ArXiv, Ogbn-Proteins, and Ogbl-Collab were provided by the benchmark (Hu et al. 2020). Specifically, for Ogbn-ArXiv, we train on papers published until 2017, validate on papers from 2018 and test on those published since 2019. For Ogbn-Proteins, protein nodes were segregated into training, validation, and test sets based on their species of origin. For Ogbl-Collab, we employed collaborations until 2017 as training edges, those in 2018 as validation edges, and those in 2019 as test edges.

E.5 More Details about Backbones

As for small- and medium-scale datasets Cora, Citeseer and PubMed, we choose the two-layer GCN/GIN/GAT networks with 512 hidden units to conduct all our experiments. As for large-scale datasets Ogbn-ArXiv, Ogbn-Proteins and Ogbl-Collab, we use the ResGCN with 28 GCN layers to conduct all our experiments.

For comparison with state-of-the-art GLT methods, we choose UGS and TGLT, which are the most efficient GLT methods to our best knowledge.

- **UGS** (Chen et al. 2021b): We utilize the official implementation from the authors. Notably, UGS was originally designed for joint pruning of model parameters and edges. Specifically, it sets separate pruning parameters for parameters and edges, namely the weight pruning ratio p_θ and the graph pruning ratio p_g . In each iteration, a corresponding proportion of parameters/edges is pruned. For a fairer comparison, we set $p_\theta = 0\%$ and $p_g \in \{5\%, 10\%\}$ to get the results of all sparsity granularity.
- **WD-GLT** (Hui et al. 2023): WD-GLT inherits the iterative magnitude pruning paradigm from UGS, so we also set $p_\theta = 0\%$ and $p_g \in \{5\%, 10\%\}$ across all datasets and backbones. The perturbation ratio α is tuned among $\{0, 1\}$. Since no official implementation is provided, we carefully reproduced the results according to the original paper.